Electronic Supplementary Material (ESI) for Dalton Transactions.

Electronic Supplementary Information

Unsymmetrical Diborane(4) Derivatives by Copper Mediated B–B Coupling

Wiebke Oschmann, Corinna Borner and Christian Kleeberg*

Institut für Anorganische und Analytische Chemie,
Technische Universität Carolo-Wilhelmina zu Braunschweig,
Hagenring 30, 38106 Braunschweig, Germany.

* Author E-mail Address: ch.kleeberg@tu-braunschweig.de

Contents

1. Additional Experimental Data

a. Reaction of 2 with (mesEn)B–Br (3d) (*in situ* NMR experiment)

In a nitrogen filled glovebox [(IDipp)Cu–O*t*Bu] (20 mg, 38 µmol, 1.0 eq) and **1a** (10 mg, 38 µmol, 1.0 eq) were combined in dry C_6D_6 (0.6 mL) and transferred into a screw-cap NMR tube. ^1H and $^{11}B\{^1H\}$ NMR spectra were recorded. After ca. 30 min **3d** (18 mg, 46 µmol, 1.3 eq) was added and ^1H and $^{11}B\{^1H\}$ NMR spectra were recorded.

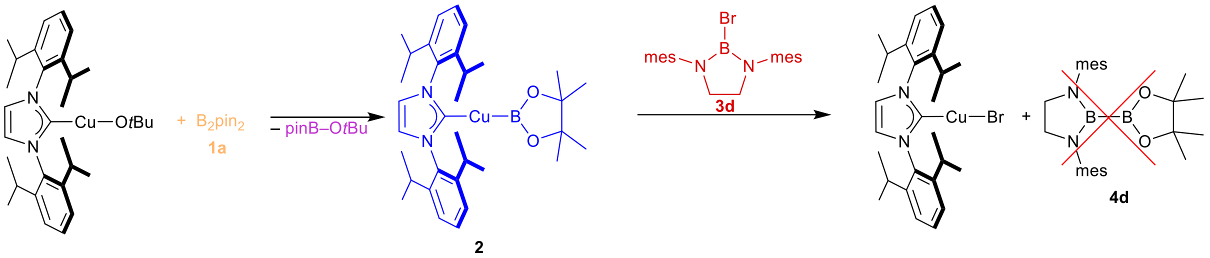

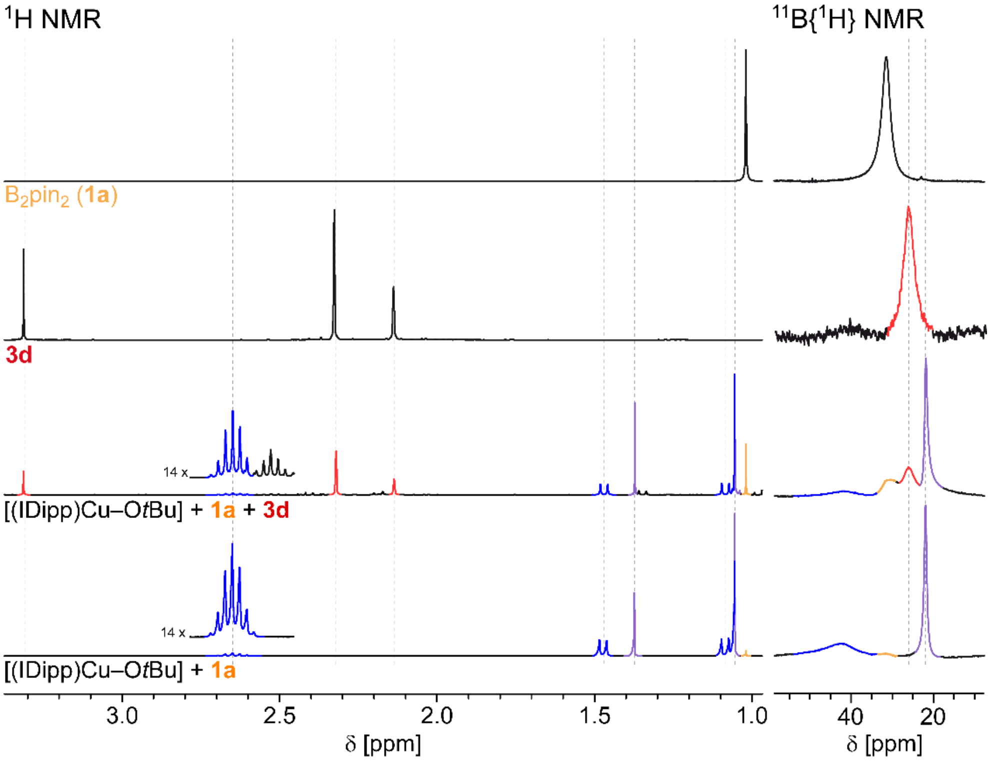

Figure S1. *In situ* NMR spectra of the reaction of **1a** with [(IDipp)Cu–O*t*Bu] to give **2** (after 30 min, bottom) and its reaction with **3a** (after 4.5 h) (middle) and of authentic samples of B_2pin_2 (**1a**) and (mesEn)B–Br (**3d**).

Result: No reaction of **3d** with **2** is observed within 4.5 h at ambient temperature.

b. Recovery of [(IDipp)CuBr] and [(IDipp)CuCl]

[(IDipp)CuBr]: From a synthesis of **5c** (0.67 mmol scale) [(IDipp)CuBr] was recovered upon filtration of the *n*-pentane extracts (287 mg, 0.54 mmol, 81%) as a pale solid (Figure S2).

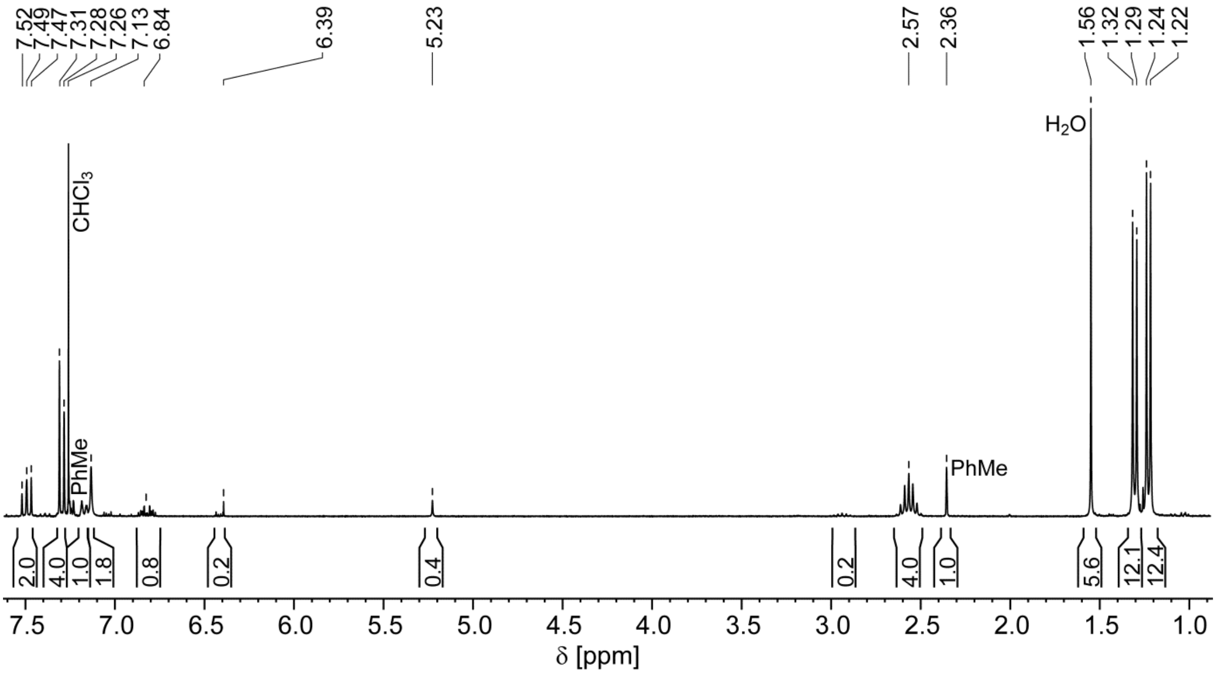

Figure S2. ^{1}H NMR spectrum of recovered [(IDipp)CuBr] (300 MHz, rt, $CDCl_3$).

The ^{1}H NMR spectrum of the obtained material (Figure S2) gives clear evidence for the presence of [(IDipp)CuBr] as the main component (literature data: δ_H($CDCl_3$): 1.24 (d, J = 6.8 Hz, 12 H, ArCHCH_3), 1.31 (d, J = 6.8 Hz, 12 H, ArCHCH_3), 2.57 (sept., J = 6.8 Hz, 4 H, ArC*H*CH_3), 7.14 (s, 2 H, NCH=), 7.30 (d, J = 7.8 Hz, 4 H, H_{Ar}), 7.50 (t, J = 7.8 Hz, 2 H, H_{Ar})).[S1] Some residual PhMe, the solvent used in the reaction (ca. 30 mol% relative to [(IDipp)CuBr]), water (the NMR was not recorded under inert conditions) and a small amount of unassigned impurities are observed.[S2]

[(IDipp)CuCl]: From four independent syntheses of **4e** and **4f** (overall 3.99 mmol of [(IDipp)CuO*t*Bu]) virtually clean [(IDipp)CuCl] was recovered upon filtration of the *n*-pentane extracts (1.87 g, 3.85 mmol, 96%) as a pale solid (Figure S3).

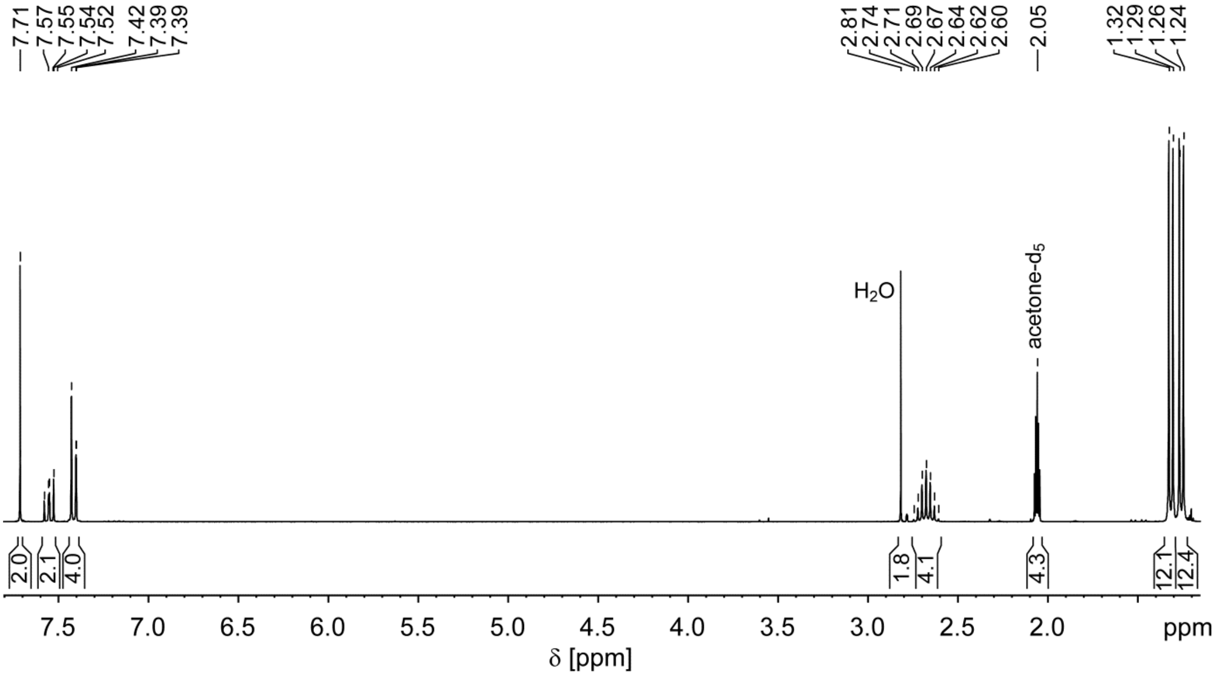

Figure S3. ^{1}H NMR spectrum of recovered [(IDipp)CuCl] (300 MHz, rt, acetone-d_6).

The ^{1}H NMR spectrum of the obtained material (Figure S3) gives clear evidence for the presence of [(IDipp)CuCl] as sole component (literature data: δ_H(acetone-d_6): 1.26–1.24 (d, J = 6.9 Hz, 12 H), 1.32–1.30 (d, J = 6.9 Hz, 12 H), 2.71–2.62 (m, 4 H), 7.41 (d, J = 7.8 Hz, 4 H), 7.54 (dd, J = 7.5, 7.2 Hz, 2 H), 7.71 (s, 2 H),).[S3]

c. Purification of neopB–Bpin (4e) by column chromatography

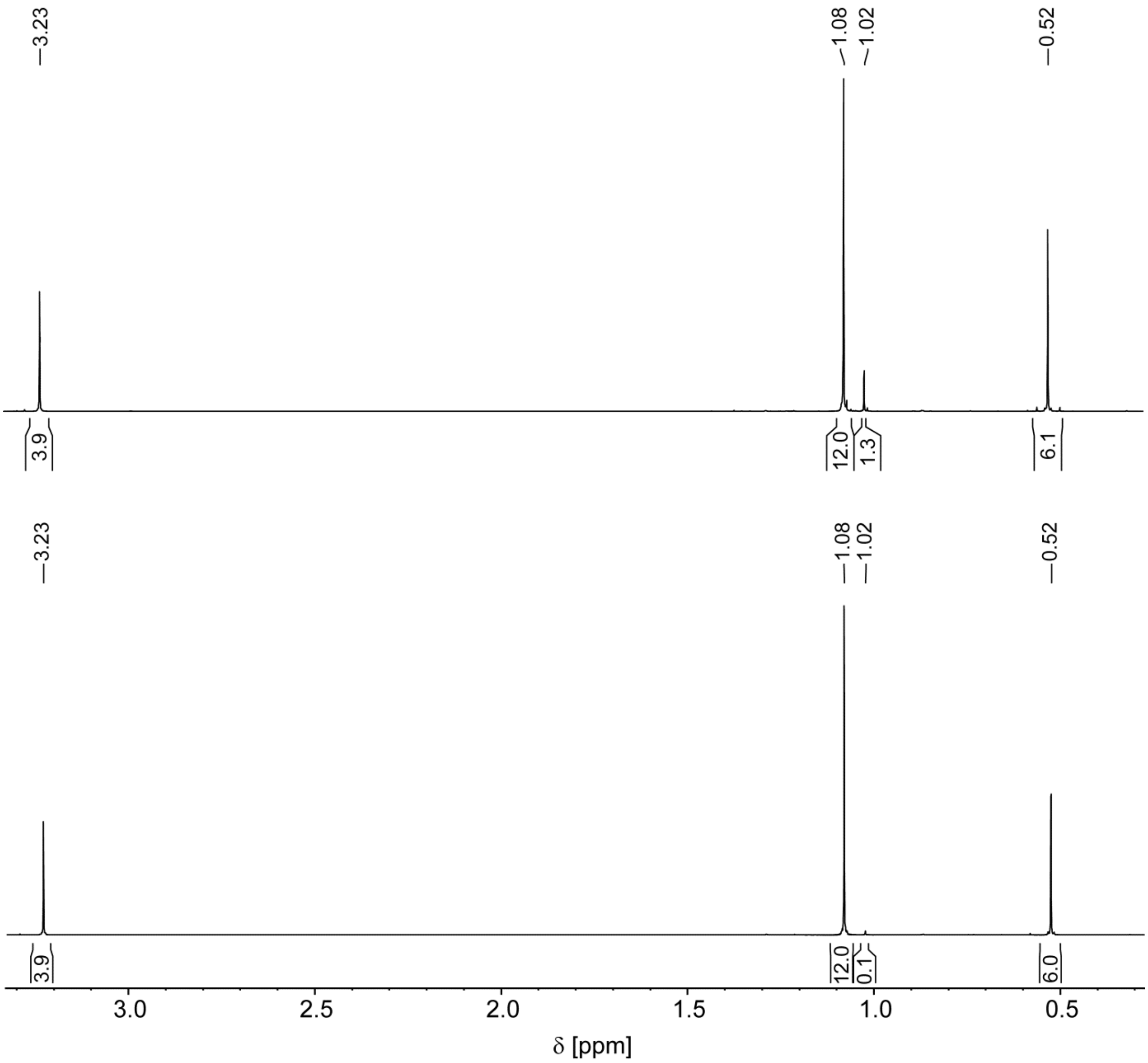

Figure S4. ^{1}H NMR spectra of **4e** before (top) and after (bottom) purification by column chromatography (300 MHz, rt, C_6D_6).

The ^{1}H NMR spectra obtained show clearly the purification of **4e** by column chromatography (Figure S4). The integrals of the Bpin signals (**4e**: 1.08 ppm, **1a**: 1.02 ppm) allow the estimation of the content of **1a** in **4e**. Whilst it amounts to 5 mol% before purification it is estimated to 0.4 mol% after column chromatography.

d. Synthesis of dmabB-Br (3g)

3g was synthesised adapting a procedure reported for (MeEn)B–Br (**3c**).[S4a] Triethylamine (1.47 mL, 1.07 g, 10.6 mmol, 2.0 eq) was dissolved in *n*-hexane (3.5 mL) and cooled to 0 °C. A solution of BBr_3 (0.51 mL, 1.33 g, 5.3 mmol, 1.0 eq) in *n*-hexane (0.7 mL) was added via a dropping funnel under vigorous stirring. The funnel was washed with *n*-hexane (1 mL) and the reaction mixture warmed to room temperature. A solution of *N*,*N'*-dimethylbenzene-1,2-diamine[S4b,c,d] (716 mg, 5.3 mmol, 1.0 eq) in *n*-hexane (2.5 mL) was added slowly and the mixture was refluxed for 3 h. The mixture was filtered over celite and washed with *n*-hexane (2 × 3 mL), the solvent was removed under vacuum to give the product as a pale pink to brown sticky solid in satisfactory purity.

Yield: 0.34 g, 3.58 mmol, 68%.

δ_H(300 MHz, C_6D_6):	2.88 (6 H, s, CH_3), 6.70 – 6.76 (2 H, m, CH_{Ar}), 7.00 – 7.04 (2 H, m, CH_{Ar}).
δ_C(75 MHz, C_6D_6):	29.2 (CH_3), 108.9 (CH_{Ar}), 119.9 (CH_{Ar}), 137.8 (C_{Ar}).
δ_B(96 MHz, C_6D_6):	24.1 (s, $\Delta w_{½}$ = 53 Hz).

2. Additional Crystallographic Data

(*i*PrEn)B–Bpin (4a): The crystal is likely to be twinned by inversion and was refined accordingly; the twin factor refined, in the absence of strong anomalous scatterer to 0.59(26). In agreement with that a likelihood analysis of the Bijvoet pairs suggests racemic twinnig:[S5]

P2(true): n/a
P3(true): $0.2\cdot10^{-17}$
P3(rac-twin): 1.000
P3(false): $0.8\cdot10^{-6}$
Hooft y: 0.62(7)
Parsons z: 0.63(6)

neopB–Bpin (4e): A disordered Bneop moiety was refined using a split atom model (0.884(3) SOF of main component), applying similarity restraints and refining a common ADP for certain disordered atom pairs (SAME, EADP).

catB–Bpin (4f): A disordered Bpin group was refined using a split atom model (0.47(1) SOF of minor component). Geometry restraints were employed (DFIX).

a. Crystal Structure Determination of 4c

Crystallisation and data collection: Compound **4c** was crystallised by *in situ* crystallisation on the diffractometer. Pure pinB-BMeEn (approx. 0.8 /mL) was enclosed in a glass capillary of 0.4 mm outer diameter. The capillary was flame sealed and glued into a brass pin that was mounted on the goniometer head. The axis of the capillary was aligned perpendicular to the X-ray beam and the part of the capillary filled with pinB-BMeEn was centred in the X-ray beam (0.5 mm dia.). The temperature was gradually (within 3 h) lowered from rt to 248 K and kept at this temperature for 20 h. At this point the pinB-BMeEn crystallised upon shock cooling with a piece of paper dipped in liquid nitrogen. Sequences of cooling to 248 K, annealing, shock cooling and reheating were repeated until the diffraction pattern indicated that a reasonably single crystalline sample had formed. Finally, the temperature was lowered to 235 K and a dataset was collected, then (after about 20 h) the temperature was lowered to 100 K and another dataset was collected.

Crystallographic data collection parameters for 4c at 235 K:

Formula	$C_{10}H_{22}B_2N_2O_2$	T (K)	235(2)
Mass (g mol^{-1})	280.02	Radiation, λ (Å)	MoKα, 0.71073
Cryst. cond.	*in situ cryst.*	μ (mm^{-1})	0.072
Cryst. size (mm^3)	0.8 × 0.4 × 0.4	Reflections:	
Crystal system	orthorhombic	all	25115
Space gr. (no.)	*Pnma* (62)	indep.	1276
Z, Z'	4, ½	obs. [$I > 2\sigma(I)$]	1102
a (Å)	7.7413(4)	2θ range (°)	2.72 – 25.02
b (Å)	11.8768(6)	Param. / Restr.	111 / 0
c (Å)	14.9725(6)	GooF on F^2	1.103
α (°)	90	R_{int}	0.0344
β (°)	90	R_1 [$I > 2\sigma(I)$]	0.0479
γ (°)	90	wR_2 (all data)	0.1369
Volume (Å^3)	1376.6(1)	peak / hole (Å^{-3})	0.203 / –0.131
D_{calcd} (Mg m^{-3})	1.080	CCDC no.	1820525

Structure discussion: At 235 K **4c** was found to crystallise in an orthorhombic space group *Pnma* with half a molecule of **4c** in the asymmetric unit situated on a mirror plane (Figure S5). The mirror plane through the atoms B1 and B2 and is perpendicular to the planar (MeEn)B moiety, however, the Bpin is disordered over two symmetry related positions, as it does not adopt mirror symmetry.

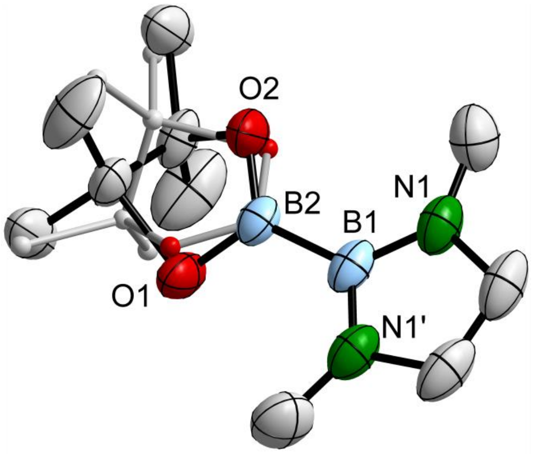

Figure S5. View of the molecular structure of **4c**. Selected distances (Å) and angles (°): B1–B2 1.709(3), B1–N1 1.405(2), B2–O1 1.402(4), B2–O2 1.318(4), N1–B1–N1’ 108.1(2), O1–B2–O2 111.9(2), τ 17.0(1).

The B–B distances of 1.709(3) Å found for **4c** at 235 K is in agreement with the 1.695(2) Å found at 100 K and also within the typical range found for diamino dialkoxy diborane(4) derivatives. The interplanar angle τ is by 3° slightly larger than at 100 K, however, this value may be impaired by the disorder; the same is true for the N/O–B distances and O–B–O/N–B–N angles that are not discussed further.

Upon cooling to 100 K a monoclinic cell in the space group $P2_1/c$ of slightly smaller volume is found. By this reduction of the crystallographic symmetry the molecular symmetry is also reduced. The individual molecules of **4c** now do not exhibit any higher molecular symmetry (Z = 4, Z' = 1). Moreover, this phase transition is associated with the occurrence of twinning; the crystal at 100 K was twinned by 180° rotation about the a* axis and was refined as a 2-component twin. The twin factor refined to 0.476(1).

b. Crystal Structure Determinations of 4e co-crystallised with B$_2$pin$_2$ (1a)

	4e[a]	$\mathbf{4e}_{0.92}\mathbf{1a}_{0.08}$[b]	$\mathbf{4e}_{0.89}\mathbf{1a}_{0.11}$[c]	$\mathbf{4e}_{0.83}\mathbf{1a}_{0.17}$[d]	$\mathbf{4e}_{0.82}\mathbf{1a}_{0.18}$[e]
Source	after chromatogr.	from crude extract	mixture **4e**:**1a** (4:1)	mixture **4e**:**1a** (2:1)	mixture **4e**:**1a** (1:1)
Cryst. cond.	C_5H_{12}, –40 °C	C_5H_{12}, –40 °C	C_5H_{12}, –40 °C	C_5H_{12}, –40 °C	C_5H_{12}, –40 °C
Composition	$C_{11}H_{22}B_2O_4$	$(C_{11}H_{22}B_2O_4)$ $(C_{12}H_{24}B_2O_4)_{0.09}$	$(C_{11}H_{22}B_2O_4)$ $(C_{12}H_{24}B_2O_4)_{0.13}$	$(C_{11}H_{22}B_2O_4)$ $(C_{12}H_{24}B_2O_4)_{0.20}$	$(C_{11}H_{22}B_2O_4)$ $(C_{12}H_{24}B_2O_4)_{0.22}$
Mass (g mol^{-1})	239.90	241.02	241.56	242.24	242.47
Cryst. size (mm^3)	0.27×0.20×0.04	0.18×0.17×0.09	0.14×0.08×0.06	0.23×0.12×0.12	0.18×0.14×0.07
Crystal system	monoclinic	monoclinic	monoclinic	monoclinic	monoclinic
Space gr. (no.)	$P2_1/c$ (14)	$P2_1/c$ (14)	$P2_1/c$ (14)	$P2_1/c$ (14)	$P2_1/c$ (14)
Z, Z'	8, 2	8, 2	8, 2	8, 2	8, 2
a (Å)	20.4725(8)	20.4063(9)	20.4494(14)	20.2409(10)	20.1037(12)
b (Å)	11.5631(4)	11.6263(5)	11.6284(8)	11.7717(4)	11.8880(6)
c (Å)	11.6719(4)	11.6803(4)	11.6718(8)	11.6993(4)	11.7240(7)
α (°)	90	90	90	90	90
β (°)	91.666(4)	92.014(4)	92.161(6)	92.725(3)	93.134(6)
γ (°)	90	90	90	90	90
Volume (Å^3)	2761.9(2)	2769.4(2)	2773.5(3)	2784.44(2)	2797.8(3)
D_{calcd} (Mg m^{-3})	1.154	1.156	1.157	1.156	1.151
T (K)	100(2)	101(2) K	100(2) K	100(2) K	100(2) K
Radiation, λ (Å)	CuK$_\alpha$, 1.54184	CuK$_\alpha$, 1.54184	CuK$_\alpha$, 1.54184	CuK$_\alpha$, 1.54184	CuK$_\alpha$, 1.54184
μ (mm^{-1})	0.667	0.667	0.667	0.666	0.663
Reflections: all	54419	49157			
indep.	5785	5034	5521	6940	6495
obs. [$I > 2\sigma(I)$]	4627	3817	3686	5924	4343
2θ range (°)	4.32 – 76.77	4.34 – 68.00	4.33 – 67.00	4.35 – 76.44	4.32 – 67.00
Param. / Restr.	354 / 19	396 / 68	412 / 48	432 / 97	450 / 73
GooF on F^2	1.043	1.039	0.985	1.083	0.999
R_{int}	0.0802	0.0758	n/a	n/a	n/a
R_1 [$I > 2\sigma(I)$]	0.0475	0.0541	0.0541	0.0690	0.0665
wR_2 (all data)	0.1354	0.1600	0.1492	0.1852	0.1880
twin factor			0.207(2)	0.271(2)	0.381(2)
peak / hole (Å^{-3})	0.377 / –0.270	0.623 / –0.209	0.437 / –0.116	0.490 / –0.175	0.496 / –0.212
CCDC no.	1820517	1820518	1820514	1820523	1820516

[a] see main text for further details. [b] The structure comprises two independent molecules one fully occupied by **4e** and the second one occupied by **4e** (SOF: 0.836(3) and **1a**. Restrains were employed (ISOR, SAME). [c] The crystal is non-merohedrally twinned by 180° rotation about the 0.95 0.00 0.31 (rec) 0.69 0.00 0.73 (dir) direction and was refined accordingly using a dataset containing only reflections with contributions of the major component. The structure contains several disordered Bpin and Bneop moieties. Split atom models were established for each disordered part employing similarity restraint (SAME) and refining only a common ADP for heavily correlating groups of atoms. The structure comprises two independent molecules one fully occupied by **4e** and the second one occupied by **4e** (SOF: 0.767(4) and **1a**. [d] The crystal is non-merohedrally twinned by 180° rotation about the *c*-axis and was refined accordingly using a dataset containing only reflections with contributions of the major component. The structure contains several disordered Bpin and Bneop moieties. Split atom models were established for each disordered part employing similarity restraint (SAME) and refining only a common ADP for heavily correlating groups of atoms. The structure comprises two independent molecules; one fully occupied by **4e** and the second one occupied by **1a** (disordered over two positions, SOF: 0.222(3), 0.109(2)) and **4e** in an overall ratio of ⅓ to ⅔. [e] The crystal is non-merohedrally twinned by 180° rotation about the *a**-axis and was refined accordingly using a dataset containing only reflections with contributions of the major component. The structure contains several disordered Bpin and Bneop moieties. Split atom models were established for each disordered part employing similarity restraint (SAME) and refining only a common ADP for heavily correlating groups of atoms. The structure comprises two independent molecules; one fully occupied by **4e** and the second one occupied by **1a** (disordered over two positions, SOF: 0.218(3), 0.144(3)) and **4e** in an overall ratio of 0.36 to 0.64.

Table S1. Crystallographic data collection parameters for **4e** and different co-crystals $\mathbf{4e}_{1-x}\mathbf{1a}_x$.

Recrystallisation of (**4e**) from the crude *n*-pentane extract of the reaction delivered **4e** co-crystallised with B$_2$pin$_2$ (**1a**). A representative crystal obtained under these conditions showed a crystallographically determined content of **1a** of 8 mol%, in reasonable agreement with the 5 mol% calculated from the NMR integration (Table

S1, crystal A). Remarkably, in the co-crystal A the individual molecules of **1a** are located selectively on one of the two sites occupied by independent molecules of **4e** (molecule B in Figure 4 and Figure S6 (left). In order to explore this co-crystallisation further single crystals were obtained under virtually identical conditions starting from different mixtures of **4e** and **1a**. Starting from molar ratios of 4:1, 2:1 and 1:1 single crystals were obtained and single crystal X-ray diffraction analysis was conducted. In all cases, co-crystallisation of **4e** with **1a** was observed, albeit with different compositions (Table S1).

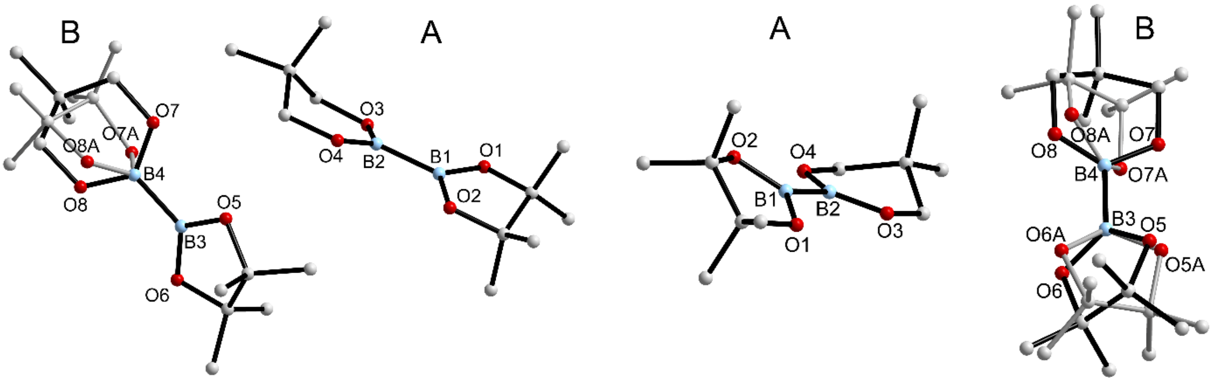

Figure S6. Views of the asymmetric units of **4e**$_{0.92}$**1a**$_{0.08}$ (left) and **4e**$_{0.89}$**1a**$_{0.11}$ (right). Selected distances (Å) and angles (°): **4e**$_{0.92}$**1a**$_{0.08}$: Molecule A: B1–B2 1.713(3), τ 17.4(1). Molecule B: B3–B4 1.717(3), τ(**4e**) 43.8(2), τ(**1a**) 77.8(9). **4e**$_{0.89}$**1a**$_{0.11}$: Molecule A: B1–B2 1.714(3), τ 20.2(8). Molecule B: B3–B4 1.723(5), τ(**4e**) 42.1(1), τ(**1a**) 85(1) (only major component (SOF: 0.944(2)) of disordered pin at B3 moiety considered).

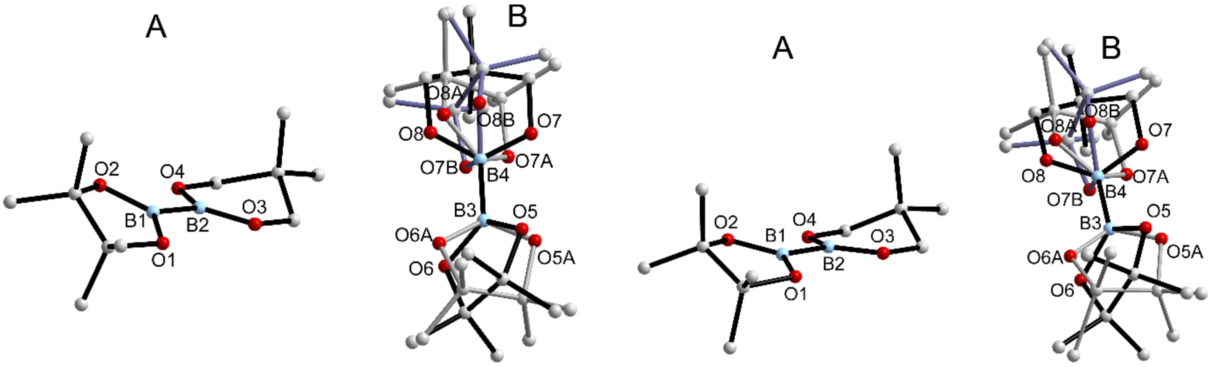

Figure S7. Views of the asymmetric units of **4e**$_{0.83}$**1a**$_{0.17}$ (left) and **4e**$_{0.82}$**1a**$_{0.18}$ (right). Selected distances (Å) and angles (°): **4e**$_{0.83}$**1a**$_{0.17}$: Molecule A: B1–B2 1.705(4), τ 15.6(9). Molecule B: B3–B4 1.725(5), τ(**4e**) 42.7(2), τ(**1a**) 89.6(5), 41.2(7) (only major component (SOF: 0.814(3)) of disordered pin moiety considered). **4e**$_{0.82}$**1a**$_{0.18}$: Molecule A: B1–B2 1.701(4), τ 13.6(1). Molecule B: B3–B4 1.722(5), τ(**4e**) 40.4(3), τ(**1a**) 89.5(4), 42.6(5) (only major component (SOF: 0.705(3)) of disordered pin at B3 moiety considered).

However, the crystallographically determined ratios of **4e**:**1a** increase indeed with increasing **4e**:**1a** ratios used in the preparation, however, even starting from a 1:1 ratio (**4e**:**1a**) only a 1:0.22 ratio is found in the co-crystal, virtually the same ratio also obtained from a 2:1 (**4e**:**1a**) ratio (Table S1). Nonetheless, structurally all these structures – including the one of pure **4e** – are closely related. In all cases only molecule B (in the structure of pure **4e**) is disordered with co-crystallised **1a**, whilst the structural parameter of molecule A remain virtually unchanged independently of the amount of co-crystallised **1a** (Figures S6 and S7). The latter may be illustrated by the small range of B–B distances of 1.701–1.714 Å with an average esd of 0.003 Å and the interplanar angle τ in a range of 13.6–20.2° with esds in the range of 0.05–0.9°.

Molecule B however shows a greater variety of geometrical parameters. Considering only to the major components of these disordered moieties the B–B distances cover a range of 1.713–1.725 Å with an average esd of 0.005 Å, hence are virtually in the same range as found for molecule A. However, it has to be considered that imperfect description of the disorder leads certainly to underestimated esds. The interplanar angle τ covers a range of 40.4–43.8°, hence, is significantly larger than those found for molecule A. In other words, **4e** adopts two distinctly different conformations and only the more twisted conformation, realised in molecule B, shows substitutional disorder with **1a** (and is also disordered in the case of pure **4e**; see main text).

The geometrical parameters of the co-crystallised **1a** may also – with all due care because of the relatively small occupancies and the associated errors – be addressed. The B–B distances are with about 1.713–1.725 Å on the long side of the range but still in agreement with the values observed for pure **1a** (1.696(5) Å, 1.707(5) Å).[S6] The interplanar angle τ varies for co-crystallised **1a** in the range of 77.8–89.6° for the major component and 41.2–42.6° for the minor component, whereas in pure **1a** angles of 1.8–35.1° are reported.[S6] This illustrates the obviously low barrier for rotation about the B–B bond in **1a**, as addressed elswhere.[S6]

The different ratios of **4e**:**1a** realised in the co-crystals are also reflected in the unit cell dimensions. Going from pure **4e** to $\mathbf{4e}_{0.82}\mathbf{1a}_{0.18}$ the length of the *a* axis decreases by 0.38 Å and the length of the *b* axis increases by about 0.32 Å, whilst the length of the *c* axis increases only slightly by 0.05 Å and also the monoclinic angle increases by

1.47° with increasing co-crystallised amounts of **1a** (noteworthy, there is a small inconstancy between $\mathbf{4e}_{0.92}\mathbf{1a}_{0.08}$ and $\mathbf{4e}_{0.89}\mathbf{1a}_{0.11}$).

c. Additional Structural Data on 5c

100 K: The dimer of catB-BMeEn shows whole molecule disorder that was refined with an appropriate split-atom model (SOF of major component: 0.951(3). The minor component was refined employing similarity restraints (SAME); due to correlation effect for the minor component a common isotropic displacement parameter was refined (0.019(4)).

250 K: The crystal was non-merohedrally twinned by 180° rotation about the [1 0 0] axis in reciprocal space respectively the [1 0 0.14] axis in direct space. The structure solution was conducted with data of one component only and the refinement was conducted as a 2-component twin (twin factor: 0.05(1)).

Temperature dependent phase transition of 5c:

	275 K	250 K	225 K	200 K		166 K	150 K	133 K	100 K	
Cryst.	**A**	**A**	**A**	**A**	**B**	**B**	**A**	**B**	**B**	**C**
a /Å	7.2678(4)	7.2394(4)	7.291(2)	7.272(3)	7.272(3)	7.255(4)	7.254(4)	7.2363(6)	7.221(2)	7.2191(6)
b /Å	12.5218(9)	12.5205(7)	24.366(4)	24.392(4)	24.371(3)	24.368(5)	24.391(9)	24.3658(7)	24.371(2)	24.358(1)
c /Å	12.8966(8)	12.8693(7)	12.632(5)	12.594(5)	12.603(4)	12.583(6)	12.574(7)	12.5612(9)	12.543(2)	12.555(1)
β /°	104.099(6)	104.126(6)	105.82(4)	105.74(4)	105.81(4)	105.76(4)	105.74(6)	105.778(8)	105.73(2)	105.723(9)
V /Å^3	1138.3(1)	1131.2(1)	2159(1)	2150(1)	2149(1)	2141(2)	2141(1)	2131.3(3)	2124.5(7)	2125.1(3)
Z, Z'	4, ½	4, ½	8, 2	8, 2	8, 2	8, 2	8, 2	8, 2	8, 2	8, 2
V/Z /Å^3	284.6	282.8	269.9	268.8	268.6	267.6	267.6	266.4	265.6	265.6

Table S2. Cell metrics in dependence of the temperature measured at three different crystals (A, B and C) as determined by single crystal X-ray diffraction.

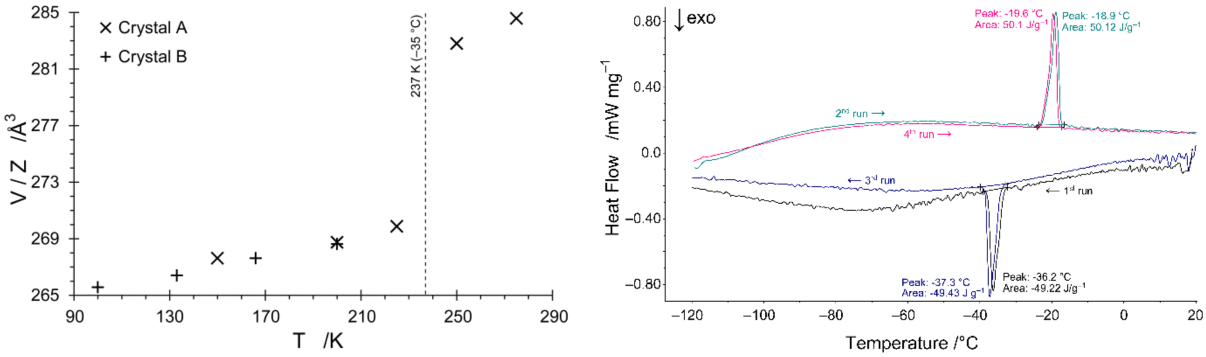

Figure S8. *Left:* Diagram showing the molecular volume with respect to monomeric **5c** (Cell Volume/Z) in dependence of the temperature. *Right:* DSC curve of **5c** (two cycles, each a. 20° C → –120 ° at 2 °C/min, b. –120° C → 20 ° at 2 °C/min, before each run 5 min at starting temperature, sample weight: 7.045 mg).

The cell parameters were determined on three independently prepared single crystals of **5c** prepared by slow evaporation of THF (crystal A and C) and C_6D_6 (crystal B), respectively. The molecular volume (as calculated from *V* / *Z*) of **5c** in the solid state reduced by 4.6% upon cooling from 250 K to 225 K (the non-hydrogen atomic volume is reduced from 17.7 Å to 16.9 Å), whilst from 225 K to 100 K a change of only 1.6% is observed (Table S2, Figure S8 left). This sudden change in molecular volume clearly indicates a phase transition; moreover, the *b* axis is doubled in the phase transition.

The crystallographic data are complemented by the DSC data indicating a reversible exothermic process upon cooling around 236 K, however, the high-temperature form is not reached until heating to 254 K (Figure S8 right). The reversibility of the phase-transition is also observed crystallographically, however, the mosaic structure of the single crystals are greatly impaired by the phase transition rendering repeated cell determinations difficult.

3. References

S1 S. Diez-González, E. C. Escudero-Adán, J. Benet-Buchholz, E. D. Stevens, A. M. Z. Slawinc and S. P. Nolan, *Dalton Trans.*, 2010, **39**, 7595.

S2 G. R. Fulmer, A. J. M. Miller, N. H. Sherden, H. E. Gottlieb, A. Nudelman, B. M. Stoltz, J. E. Bercaw and K. I. Goldberg, *Organometallics*, 2010, **29**, 2176.

S3 J. Chun, G. Jung, H. J. Kim, M. Park, M. S. Lah and S. U. Son, *Inorg. Chem.*, 2009, **48**, 6353.

S4 (a) T.-T. Wang, P. J. Busse and K. Niedenzu, *Inorg. Chem.*, 1970, **9**, 2150; (b) N. Proust, J. C. Gallucci and L. A. Paquette, *J. Org. Chem.*, 2009, **74**, 2897; (c) E. Hasegawa, T. Seida, N. Chiba, T. Takahashi and H. Ikeda, *J. Org. Chem.*, 2005, **70**, 9632; (d) T. Vlaar, R. C. Cioc, P. Mampuys, B. U. W. Maes, R. V. A. Orru and E. Ruijter, *Angew. Chem. Int. Ed.*, 2012, **51**, 13058.

S5 R. W. W. Hooft, L. H. Straver and A. L. Spek, *J. Appl. Cryst.*, 2008, **41**, 96.

S6 M. Eck, S. Würtemberger-Pietsch, A. Eichhorn, J. H. J. Berthel, R. Bertermann, U. S. D. Paul, H. Schneider, A. Friedrich, C. Kleeberg, U. Radius and T. B. Marder, *Dalton Trans.*, 2017, **46**, 3661.